

Inelastic-scattering rate on thermal conductivity of a $d_{x^2-y^2}$ superconductor

E. Schachinger

Institut für Theoretische Physik, Technische Universität Graz, A-8010 Graz, Austria

J. P. Carbotte

Department of Physics and Astronomy, McMaster University, Hamilton, Ontario, Canada L8S 4M1

(Received 8 January 1998)

We calculate the electronic component of the thermal conductivity of a $d_{x^2-y^2}$ superconductor. We use a formalism in which the inelastic scattering is modeled explicitly through a spectral density which describes the fluctuation spectrum responsible for the superconducting transition and also for the large inelastic scattering observed in the normal state above T_c . The feedback effect of superconductivity on the spectral density is modeled by a low-frequency cutoff. For values of parameters used to successfully fit the measured microwave peak in pure and Zn- and Ni-doped Y-Ba-Cu-O we obtain good agreement with the experiment for the thermal conductivity. The effect of resonant impurity scattering is also considered, as is the zero-frequency conductivity, the Lorenz number, and the effect on these of the renormalization due to the inelastic scattering. [S0163-1829(98)00621-3]

I. INTRODUCTION

It is now widely accepted that the large peak observed¹⁻⁴ around $T=40$ K in the microwave response of optimally doped $\text{YBa}_2\text{Cu}_3\text{O}_{6.95}$ (YBCO) as a function of temperature is due to the collapse of the inelastic-scattering rates because of the onset of superconductivity. The mechanism envisaged is a feedback in which the fluctuation spectrum involved in the superconducting transition becomes gapped as a result of the gapping of the electronic spectrum. Such an effect should be generic to electronic mechanisms, but the exact detail will depend on microscopic details such as energy gap symmetry and the fluctuations involved. A rapid reduction in the scattering rate as the temperature is lowered through $T=T_c$ has also been measured in infrared⁵ studies and it has been suggested to be responsible for a large peak observed in the thermal conductivity.⁶ In this case some assumptions need to be made about the relative amount of the total thermal current coming from electrons as opposed to the phonons. Original interpretations of the thermal conductivity peak involved phonons.⁷

In this paper we use solutions of generalized Eliashberg-like equations for a d -wave superconductor which include inelastic scattering through a spectral density. The parameters of the spectral density are all fixed through our previous study of the microwave peak.⁸ No new parameters need to be introduced. From our d -wave gap solutions we calculate the electronic thermal conductivity in the superconducting state. The formulas used are standard strong-coupling formulas⁹⁻¹¹ which include the inelastic scattering, and which we have generalized to also include the gap symmetry of the $d_{x^2-y^2}$ type. There already exists a considerable literature on the thermal conductivity in exotic pairing states.¹²⁻¹⁴ All are within a BCS framework. The calculations were originally applied to heavy fermions¹⁵ but have been adapted recently to YBCO.¹⁶ In this last case an attempt is also made to include approximately into the BCS framework some inelastic scattering. This is accomplished through the introduction of a

temperature-dependent elastic-scattering rate modeled from spin-fluctuation theory.

Our own approach here is very different. The inelastic scattering is introduced through a spectral density that describes the fluctuation spectrum involved in the superconductivity which we take here for definiteness to be the antiferromagnetic spin fluctuations, although other forms of the spectral density could be used. In the case of the infrared conductivity, the generalized optical scattering rate which results from our model spectral density were indeed found to be in qualitative and semiquantitative agreement with experiment. In the normal state the model correctly gives a nearly linear temperature dependence for the scattering as well as a quasilinear ω dependence. The scattering rate is of the order of ω over a large range of energy as is observed. To include in the formalism the effect of the collapse of the inelastic scattering on entering the superconducting state a low-frequency cutoff ω_c , is introduced. This simulates the effect of the onset of superconductivity on the spectral density and the cutoff is taken to be temperature dependent and vary in the same way as the BCS gap. To obtain agreement with the microwave data in a pure twinned crystal of YBCO, ω_c at zero temperature is fixed at a value of $2.1T_c$. Further, in our microwave work the strong-coupling parameter T_c/ω_{\log} was fixed at a value of 0.31. This value was required to get the correct amount of inelastic scattering observed in the normal state just above T_c . In terms of the spin-fluctuation energy scale, this corresponds to $\omega_{\text{sf}} \approx 30$ meV which is a value quite typical of the oxides. The only other important parameter of the theory is the electron spin-fluctuation coupling which was simply adjusted to get the measured value of T_c taken 100 K as typical of the cuprates so that this too is not variable.

In Sec. II we specify the basic Eliashberg-like equations used in our work and the formula for the thermal conductivity is given. In Sec. III we discuss our results and Sec. IV presents our conclusions.

II. FORMALISM

The basic gap equations for a d -wave superconductor with inelastic scattering included through a spectral density

$I^2F(\Omega)$, which describes the bosons exchanged, have been given before. They are fundamental for all the work to be discussed and take the form:^{8,17–21}

$$\begin{aligned} \tilde{\Delta}(\nu+i\delta;\theta) = & i\pi T g \sum_{m=0}^{\infty} \cos(2\theta) [\lambda(\nu-i\omega_m) + \lambda(\nu+i\omega_m)] \left\langle \frac{\cos(2\theta') \tilde{\Delta}(i\omega_m; \theta')}{\sqrt{\tilde{\omega}^2(i\omega_m) + \tilde{\Delta}^2(i\omega_m; \theta')}} \right\rangle' \\ & + i\pi \int_{-\infty}^{\infty} dz \cos(2\theta) I^2F(z) [n(z) + f(z-\omega)] \left\langle \frac{\cos(2\theta') \tilde{\Delta}(\nu-z+i\delta; \theta')}{\sqrt{\tilde{\omega}^2(\nu-z+i\delta) - \tilde{\Delta}^2(\nu-z+i\delta; \theta')}} \right\rangle', \end{aligned} \quad (1)$$

and in the renormalization channel

$$\begin{aligned} \tilde{\omega}(\nu+i\delta) = & \nu + i\pi T \sum_{m=0}^{\infty} [\lambda(\nu-i\omega_m) - \lambda(\nu+i\omega_m)] \left\langle \frac{\tilde{\omega}(i\omega_m)}{\sqrt{\tilde{\omega}^2(i\omega_m) + \tilde{\Delta}^2(i\omega_m; \theta')}} \right\rangle' + i\pi \int_{-\infty}^{\infty} dz I^2F(z) [n(z) + f(z-\omega)] \\ & \times \left\langle \frac{\tilde{\omega}(\nu-z+i\delta)}{\sqrt{\tilde{\omega}^2(\nu-z+i\delta) - \tilde{\Delta}^2(\nu-z+i\delta; \theta')}} \right\rangle' + i\pi \Gamma^+ \frac{\Omega(\nu)}{c^2 + D^2(\nu) + \Omega^2(\nu)} \end{aligned} \quad (2)$$

with $\omega_m = \pi T(2n+1)$, $n=0, \pm 1, \pm 2, \dots$, $\langle \dots \rangle$ the angular average over θ , and

$$\lambda(\nu) = - \int_{-\infty}^{\infty} d\Omega \frac{I^2F(\Omega)}{\nu - \Omega + i0^+}, \quad (3)$$

$$D(\nu) = \left\langle \frac{\tilde{\Delta}(\nu+i\delta; \theta)}{\sqrt{\tilde{\omega}^2(\nu+i\delta) - \tilde{\Delta}^2(\nu+i\delta; \theta)}} \right\rangle, \quad (4)$$

$$\Omega(\nu) = \left\langle \frac{\tilde{\omega}(\nu+i\delta)}{\sqrt{\tilde{\omega}^2(\nu+i\delta) - \tilde{\Delta}^2(\nu+i\delta; \theta)}} \right\rangle. \quad (5)$$

Equations (1) and (2) are a set of two nonlinear coupled equations for the pairing potential $\tilde{\Delta}(\nu+i\delta; \theta)$ and the normalized frequencies $\tilde{\omega}(\nu+i\delta)$ with the gap:

$$\Delta(\nu+i\delta; \theta) = \nu \frac{\tilde{\Delta}(\nu+i\delta; \theta)}{\tilde{\omega}(\nu+i\delta)}, \quad (6)$$

or if the renormalization function $Z(\nu)$ is introduced in the usual way as $\tilde{\omega}(\nu+i\delta) = \nu Z(\nu)$ then

$$\Delta(\nu+i\delta) = \frac{\tilde{\Delta}(\nu+i\delta; \theta)}{Z(\nu)}. \quad (7)$$

Here, θ is an angle on the two-dimensional circular Fermi surface, ν is a real frequency, and δ is a positive infinitesimal 0^+ . To arrive at these equations a separable (in the angular part) model was used for the pairing potential. In the pairing channel it has the form $g \cos(2\theta) I^2F(\Omega) \cos(2\theta')$ with g a constant and $I^2F(\Omega)$ being the pairing spectral density. This leads to a gap proportional to $\cos(2\theta)$ by arrangement. No other anisotropies are included and we note that the renor-

malization channel (2) is isotropic with the same spectral density $I^2F(\Omega)$ as in Eq. (1) but with no g value. In general a different form of the spectral density could come into Eqs. (1) and (2) but here, for simplicity, we have used the same form but allowed for the possibility that they do not both have the same magnitude, i.e., g need not be equal to one. We will present results only for $g=0.8$ but we have explored other values and found no new physics. These equations can be considered as a minimum set that goes beyond a BCS approach to include approximately the inelastic scattering which is known to be very strong in the cuprate superconductors. In the normal state at T around T_c the inelastic-scattering rate often varies linearly in T as it does in our theory and is of the order of a few times T_c . These facts constrain somewhat the form of the spectral density $I^2F(\Omega)$ as will be discussed later.

In Eq. (2) the impurity scattering rate is proportional Γ^+ and comes in only in the renormalization channel because we have assumed a pure d -wave model for the gap with zero average over the Fermi surface. This is expected to be the case in a tetragonal system. If one wishes to include an s -wave part to the gap to treat an orthorhombic system, a new impurity term would now enter Eq. (1) for $\tilde{\Delta}$. It would have the same form as the last term of Eq. (2) but with $\Omega(\nu)$ in the numerator replaced by $D(\nu)$, a quantity which is strictly zero for the pure d -wave symmetry. The parameter c in the elastic-scattering part of Eq. (2) is zero for resonant or unitary scattering and infinity in the Born approximation, i.e., weak scattering limit. In this case the entire impurity term reduces to the form $i\pi t^+ \Omega(\nu)$ with c absorbed into t^+ . For intermediate coupling c is finite. The thermal factors appear in Eqs. (1) and (2) through the Bose and Fermi distribution $n(z)$ and $f(z)$, respectively.

To summarize, the parameters in the set of equations (1)–(5) are $g=0.8$ and, not of great importance, the spectral den-

sity $I^2F(\Omega)$, and the impurity parameter Γ^+ (unitary limit) or t^+ (Born limit). In our previous work on the infrared conductivity⁸ we used a model for the spectral density $I^2F(\Omega)$ motivated by a spin-fluctuation mechanism with a spectral density of the form

$$I^2F(\Omega) = I^2 \frac{\Omega/\omega_{sf}}{1 + (\Omega/\omega_{sf})^2}, \quad (8)$$

with ω_{sf} the spin-fluctuation frequency. This form has only two parameters which can be fit to experiment. First the value of I^2 can be determined upon solution of the gap equations (1) and (2) linearized in $\tilde{\Delta}$ at $T=T_c$ to get a value of

$T_c = T_{c0} = 100$ K. This value is taken to be typical of the oxides. At the same time, to get an inelastic-scattering rate in the normal state just above T_c of the order of a few T_c , we need to chose $\omega_{sf} = 30$ meV in Eq. (8) and this gives a strong-coupling index²² of $T_c/\omega_{log} = 0.31$. No parameters remain. When dealing with impurities we can either quote the value of Γ^+ used or the corresponding reduction in the critical temperature induced by the impurity scattering; but this is not a new parameter.

In the notation of our previous papers on the ac optical conductivity,^{8,23} the formula for the electronic thermal conduction can be written as

$$\kappa_{ab,e}(T) = \frac{2N(0)v_F^2}{T^2} \int_0^\infty \frac{d\nu\nu^2}{\cosh^2(\nu/2T)} \left\langle \frac{1 + N_1^2(\nu; \theta) + N_2^2(\nu; \theta) - P_1^2(\nu; \theta) - P_2^2(\nu; \theta)}{E_2(\nu; \theta)} \right\rangle, \quad (9)$$

$$E(\nu; \theta) = \sqrt{\tilde{\omega}^2(\nu + i\delta) - \tilde{\Delta}^2(\nu + i\delta; \theta)}, \quad (10)$$

$$N(\nu; \theta) = \frac{\tilde{\omega}(\nu + i\delta)}{E(\nu; \theta)}, \quad (11)$$

$$P(\nu; \theta) = \frac{\tilde{\Delta}(\nu + i\delta; \theta)}{E(\nu; \theta)}. \quad (12)$$

Here, T is the temperature, $N(0)$ is the unknown, single-spin quasiparticle density of states at the Fermi surface, and v_F is the Fermi velocity. The formula is valid in two dimensions, and it has the same general form as the formula given by Schachinger *et al.*⁸ for the zero-frequency limit of the real part of the ac conductivity of a d -wave strong-coupling superconductor which was

$$\begin{aligned} \sigma_1(0, T) = & \frac{e^2 N(0) v_F^2}{2} \left\langle \frac{1}{2T} \int_0^\infty \frac{d\nu}{\cosh^2(\nu/2T)} \frac{1 + N_1^2(\nu; \theta) + N_2^2(\nu; \theta) + P_1^2(\nu; \theta) + P_2^2(\nu; \theta)}{2E_2(\nu; \theta)} \right. \\ & - \frac{1}{4T} \int_0^\infty \frac{d\nu}{\cosh^2(\nu/2T)} \frac{1}{E_1^2(\nu; \theta) + E_2^2(\nu; \theta)} \{ 2E_1(\nu; \theta) [N_1(\nu; \theta)N_2(\nu; \theta) + P_1(\nu; \theta)P_2(\nu; \theta)] \\ & \left. + E_2(\nu; \theta) [1 - N_1^2(\nu; \theta) + N_2^2(\nu; \theta) - P_1^2(\nu; \theta) + P_2^2(\nu; \theta)] \right\rangle. \quad (13) \end{aligned}$$

In the above, the indices 1 and 2 stand for the real and imaginary parts, respectively. Also, e is the charge on the electron. Both formulas, for $\kappa_{ab,e}$ and for σ_1 , greatly simplify when retardation effects are ignored and a BCS limit is taken. This is not justified when the strong-coupling index $T_c/\omega_{log} = 0.31$ which is a very strong-coupling case,²² and we can only proceed numerically.

III. RESULTS

In Fig. 1 we show the reduced temperature T/T_c , variation of the in-plane thermal conductivity obtained in the pure case, i.e., only the inelastic scattering is included through the spectral density (8) and the elastic-impurity-scattering rate is set to zero ($\Gamma^+ = 0$) in Eq. (2). The dotted line is without a low-energy cutoff in the spectral density while the solid curve includes it. The application of this cutoff clearly has

dramatic effects on the resulting electronic thermal conductivity, changing its value by an order of magnitude in the region of the peak which falls at a reduced temperature value of slightly less than $T/T_c = 0.15$. As the temperature increases towards T_c the low-frequency cutoff in the spectral density which models the reaction of the fluctuation spectrum to the onset of superconductivity, is assumed to follow the same temperature dependence as does the BCS gap and so decreases and is zero at T_c . Thus, the solid and the dotted curve meet at $T = T_c$. It is clear from these curves that, for the pure system with no elastic impurity component, the peak in the thermal conductivity is very sensitive to the low-frequency part of the spectral density $I^2F(\Omega)$ and is a good probe for such excitations. In the best untwinned crystal samples of YBCO the residual scattering is generally believed to be small. For twinned crystals there can be some additional background scattering but we have previously

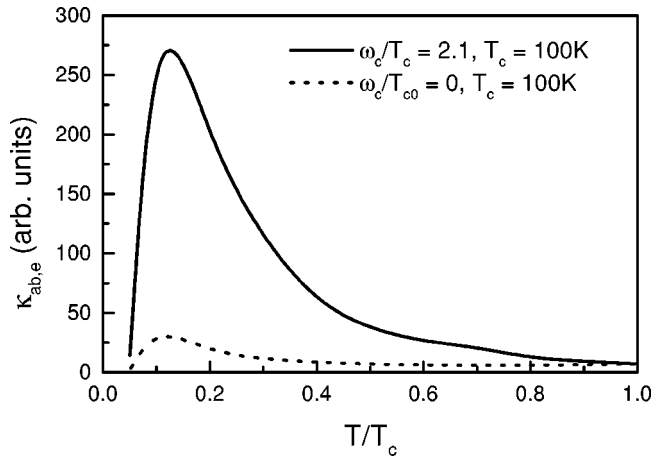


FIG. 1. In-plane electronic thermal conductivity $\kappa_{ab,e}(T)$ in arbitrary units as a function of the reduced temperature T/T_c for a pure system ($T_c = 100$ K) with inelastic scattering included. The solid curve applies to the case when a low-frequency cutoff ($\omega_c = 2.1T_c$) is introduced in the spectral density so as to simulate the effect of the superconducting transition on the fluctuation spectrum. The dotted curve involves no cutoff. The differences between the curves are dramatic.

quite successfully modeled this with a small amount of elastic Born scattering. The effect of this residual scattering on the height of the thermal conductivity peak around $T/T_c \approx 0.15$ is large and the impurities also shift the peak noticeably towards higher reduced temperature values. This is illustrated in Fig. 2 (top frame) where the effect of Born impurity scattering [i.e., $c \rightarrow \infty$ in the impurity term of Eq. (2)] is discussed. What is shown is the ratio of $\kappa_{ab,e}(T)$ to its value at $T = T_{c0}$. For the lowest impurity concentration presented in this figure, $t^+/T_{c0} = 0.0048$ (dashed curve) the peak's height is still of the order of 10 in these normalized units but has been reduced by a factor of 2 over the pure crystal case (solid curve). As the impurity concentration is increased the curves reduce further in magnitude and the peak shifts towards higher reduced temperatures. For the short dashed curve the corresponding critical temperature value is 95 K so that in this case there are enough impurities for the critical temperature to decrease by 5 K. The effect of resonant scattering is shown in the bottom frame of Fig. 2. We see that in this case the peak is more attenuated as compared to the corresponding Born case but the trends are similar. We have also done calculations for intermediate values of c , namely for $c = 0.5$ which is a value used to model the effect of Ni impurities in our previous work²³ on the microwave conductivity. The results are close to the $c = 0$ limit (resonant scattering case).

Without the introduction of any new parameters our theoretical results are scaled to meet the electronic thermal conductivity measured by Matsukawa *et al.*²⁴ (sample 3) as shown in Fig. 3. The open triangles are data for twinned crystals and the solid curve is our theoretical result. All microscopic parameters in the numerical work are the same as used in the case of the microwave.²³ To get the solid curve which fits the data well, a low-frequency cutoff was also included with $\omega_c = 2.1T_c$ at $T = 0$. Without the cutoff the dotted curve is obtained. It shows no agreement with the data so that the electronic thermal conductivity is strongly af-

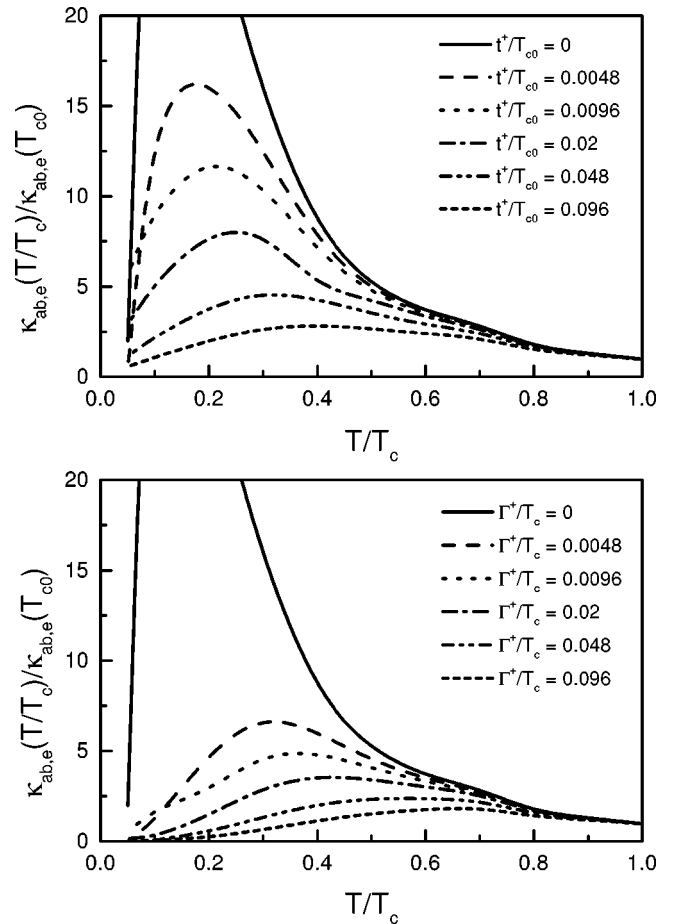


FIG. 2. In-plane electronic thermal conductivity $\kappa_{ab,e}(T)$ normalized to its value at $T_{c0} = 100$ K as a function of the reduced temperature T/T_c . In the top and the bottom frame the solid curve is for the pure case with only inelastic scattering included and the others include an additional contribution from elastic impurity scattering. In the top frame the weak scattering limit, i.e., Born approximation is made. The various curves are labeled by the value of t^+/T_{c0} employed. The peak is depressed with increasing values of t^+/T_{c0} and shifted towards higher temperatures. The bottom frame, on the other hand, is for elastic impurity scattering in the resonant limit. The various curves are labeled by the value of Γ^+/T_{c0} employed. Resonant scattering reduces the peak more rapidly than the corresponding Born case with the same value for the scattering parameter.

ected by the cutoff and thus is as sensitive a probe of the feedback effect of superconductivity on the fluctuation spectrum as is the microwave data. In Fig. 3 we have adjusted the scale on our calculations, which is arbitrary, to fit the data at the point indicated by the arrow and thus an absolute scale in units of mW/cm K applies. To set the scale theoretically the value for the combination of the free-electron density of states and Fermi velocity in Eq. (9) is needed. This is not known and thus a fit to one data point was needed. Finally, in obtaining Fig. 3 the same amount of Born residual scattering was used as required to get a good fit to microwave data in twinned samples. Thus, no new parameters or any adjustment of any kind was needed to get the fit found for the thermal conductivity shown in Fig. 3.

A quantity closely related to the thermal conductivity which is also a zero-frequency property is the $\nu \rightarrow 0$ limit of

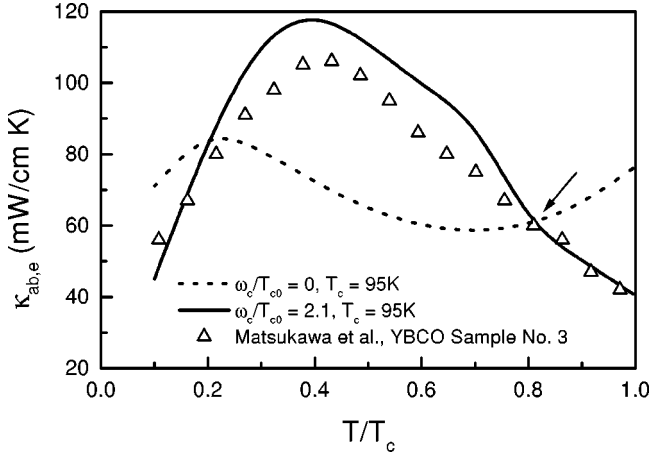


FIG. 3. The in-plane electronic thermal conductivity $\kappa_{ab,e}(T)$ in units of mW/cm K as a function of the reduced temperature T/T_c . The solid curve is the result of our calculations using the same parameters for the microscopic quantities involved as were used in our previous calculations of the microwave peak in YBCO. The open triangles are the data of Matsukawa *et al.* (Ref. 24) and are seen to agree well with our calculations. The scale of the theoretical $\kappa_{ab,e}$ was adjusted to fit the point indicated by the arrow. The dotted line is a theoretical calculation without low-frequency cutoff on the fluctuation spectrum. It disagrees strongly with the data.

the real part of the optical conductivity in the superconducting state, i.e., $\sigma_1(\nu=0, T)$ of formula (13). This quantity is closely related to the microwave conductivity. Results are shown in Fig. 4. The top frame gives the ratio of the conductivity at T normalized to the pure single-crystal value at T_{c0} . The normalization has been chosen for easy comparison with the data of Fig. 2 on the thermal conductivity. Only the resonant impurity case is shown. The top frame is without a low-frequency cutoff and the bottom frame is with. Again it is clear that the cutoff has a very large effect on the zero-frequency limit of the dc conductivity. Not only is the size of the peak strongly affected, its position is also changed from $T/T_c \approx 0.2$ to $T/T_c \approx 0.4$. This is different from the case of $\kappa_{ab,e}$ which shows little change in peak position with the cutoff value. The effect of impurity scattering in the unitary limit is similar on σ_1 as on $\kappa_{ab,e}$. Also $\sigma_1(\nu=0, T)$ is not very different from the microwave conductivity when enough impurities are present.

The comparison between thermal and electrical conductivity can be presented in a different way through the Wiedemann-Franz law or Lorenz number L . We define

$$L(T) = \frac{\kappa_{ab,e}(T)}{\sigma_1(T)T} \quad (14)$$

with the free-electron value of L equal to $L_0 = \pi^2/3(k_B/e)^2$. Figure 5 shows our results for the temperature dependence of $L(T)/L_0$ in a case which includes enough unitary impurity scattering for T_c to have dropped from T_{c0} by 5 K to 95 K. The solid curve includes the low-frequency cutoff in the spectral density and the dotted curve is without such a cutoff. We see large differences in size and also in position of the peak. At T_c both curves meet because at this temperature no low-frequency cutoff is in effect. Therefore, the electronic thermal conductivity reflects the

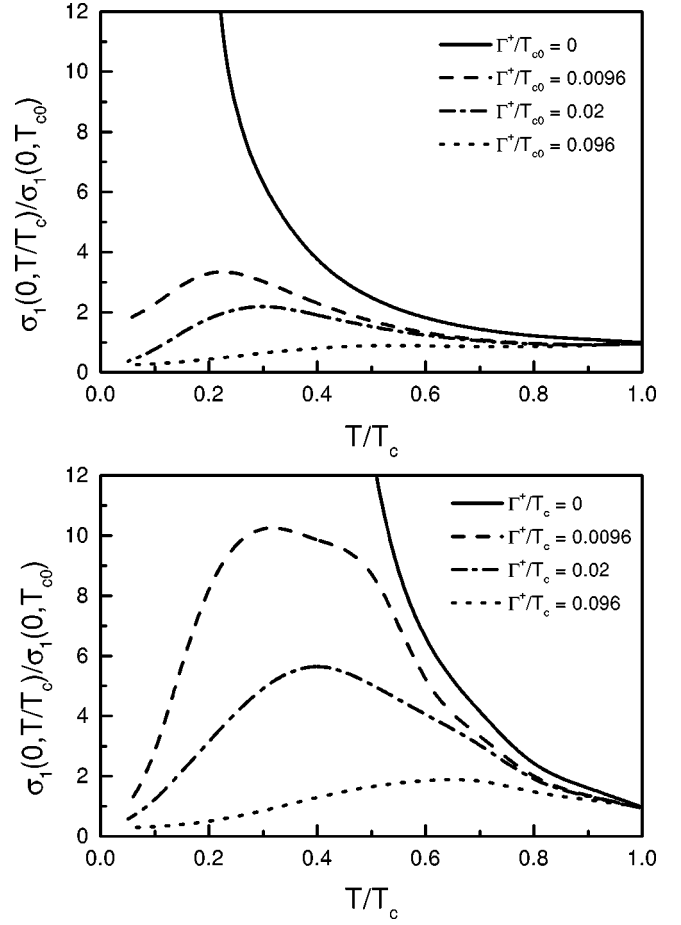


FIG. 4. The zero-frequency limit of the real part of the optical conductivity $\sigma_1(0, T/T_c)$ normalized to its value at T_{c0} (the critical temperature of the pure system) as a function of the reduced temperature T/T_c . In top frame no low-frequency cutoff has been applied to the fluctuation spectrum while in the bottom frame it has. The solid curve is for the pure case—only inelastic scattering, no elastic impurity scattering. The dashed curve is for $\Gamma^+/T_{c0} = 0.0096$ ($T_c = 99.5$ K) and the dotted one for $\Gamma^+/T_{c0} = 0.096$ ($T_c = 95$ K) with Γ^+ a measure of the elastic-scattering rate in the resonant scattering limit.

full influence of the inelastic scattering due to the spin-fluctuation spectrum (8) and L/L_0 is necessarily smaller than one. Our fit to the microwave data by Bonn *et al.*² resulted in a dc conductivity at T_c of $\sigma_1(0, T_c) = 2.56 \times 10^6 (\Omega\text{m})^{-1}$, our rescaling to the thermal data (Fig. 3) gives $\kappa_{ab,e}(T_c) = 4.1$ W/mK, and this combines according to Eq. (14) to $L(T_c) = 1.73 \times 10^{-8} \text{ W}\Omega/\text{K}^2$, well within the range of $1.2 - 2.0 \times 10^{-8} \text{ W}\Omega/\text{K}^2$ given by Hirschfeld and Putikka.¹⁶ While the microwave conductivity and thermal conductivity data are on different samples and so the unknown scaling factors $N(0)v_F^2$ in Eqs. (9) and (13) could be different, we find they differ only by less than 3% effectively from our theoretical value which does not involve this prefactor. This is quite remarkable.

At the lowest temperature shown the curves meet and we now discuss the low-temperature limit of this quantity which is particularly interesting and leads to universal limits in the case of resonant scattering.²⁵⁻²⁸ These limits have been discussed before only within the BCS weak-coupling formalism. This formalism is mathematically much less complex

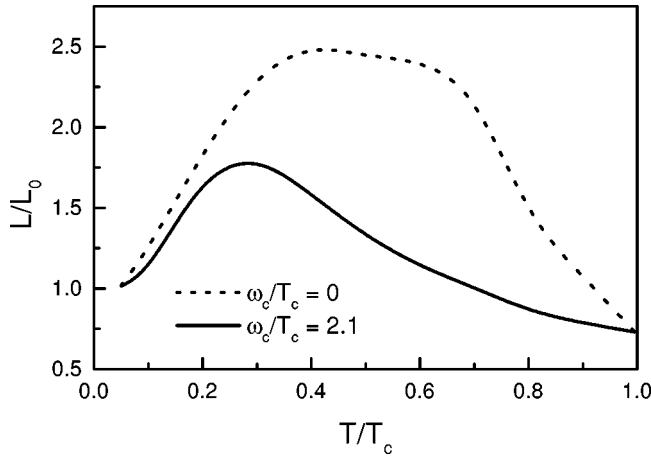


FIG. 5. The ratio of the Lorenz number L to its free-electron value as a function of the reduced temperature T/T_c . Enough impurity scattering was used to reduce the critical temperature from 100 to 95 K. The solid curve results when a low-frequency cutoff is applied to the fluctuation spectrum, while the dotted curve is without cutoff. It is clear that the inelastic scattering can have a large effect on L even when impurities are present.

than the one employed here. Our formulas are more general and include inelastic scattering but must reduce in the appropriate limit to the BCS case and they do.

We begin with the reduction of formula (9) for the thermal conductivity. In the limit of $T \rightarrow 0$ the thermal factor is highly peaked around $\nu = 0$ and we can ignore the frequency dependence in the factors that enter the average over the angle indicated by the symbol $\langle \dots \rangle$. We replace these by their normalized BCS limits

$$E(\nu=0; \theta) = E(\theta) = \sqrt{\tilde{\omega}^2(\nu=0) - \tilde{\Delta}^2(\nu=0; \theta)}, \quad (15)$$

$$N(\nu=0; \theta) = N(\theta) = \frac{\tilde{\omega}(\nu=0)}{E(\theta)}, \quad (16)$$

$$P(\nu=0; \theta) = P(\theta) = \frac{\tilde{\Delta}(\nu=0; \theta)}{E(\theta)}, \quad (17)$$

and obtain

$$\frac{\kappa_{ab,e}(T)}{T} = \frac{N(0)v_F^2}{T^2} \left\langle \frac{1 + N_1^2(\theta) + N_2^2(\theta) - P_1^2(\theta) - P_2^2(\theta)}{E_2(\theta)} \right\rangle. \quad (18)$$

Now, in the resonant scattering limit with $\nu \rightarrow 0$ we take $\tilde{\omega} \approx a\nu + i\gamma$ and so $\tilde{\omega}(\nu=0) \approx i\gamma$, where γ is the self-consistent scattering rate. In this limit

$$E_1(\theta) = N_2(\theta) = P_1(\theta) = 0,$$

and with $\tilde{\Delta}(0, \theta) \equiv \tilde{\Delta}_0(\theta)$,

$$E_2(\theta) = \sqrt{\gamma^2 + \tilde{\Delta}_0^2(\theta)}, \quad (19)$$

$$N_1(\theta) = \frac{\gamma}{E_2(\theta)}, \quad (20)$$

$$P_2(\theta) = -\frac{\tilde{\Delta}_0(\theta)}{E_2(\theta)}. \quad (21)$$

After simple algebra we get the well-known result of the BCS theory:

$$\frac{\kappa_{ab,e}(T)}{T} \Big|_{T \rightarrow 0} = \frac{N(0)v_F^2}{2} \frac{\pi^2}{3} \left[\frac{1}{\gamma} g(\gamma) - \frac{dg(\gamma)}{d\gamma} \right] \quad (22)$$

with

$$g(\gamma) = \gamma \left\langle \frac{1}{\sqrt{\gamma^2 + \tilde{\Delta}_0^2(\theta)}} \right\rangle. \quad (23)$$

Note that it is $\tilde{\Delta}_0(\theta)$ that enters Eq. (23) and not the gap $\Delta_0(\theta)$ of BCS theory. Using the familiar $\lambda^{\theta\theta}$ model²² for the interactions $\lambda(z)$ in Eqs. (1) and (2), $\tilde{\Delta}_0(\theta) = \Delta_0 \cos(2\theta)(1 + \lambda)$ where λ is the mass-renormalization parameter associated with the spectral density $I^2F(\Omega)$. Evaluation of Eq. (23) in the standard way gives

$$\frac{\kappa_{ab,e}(T)}{T} \Big|_{T \rightarrow 0} = \frac{N(0)v_F^2}{2} \frac{\pi}{3} \frac{2}{\Delta_0(1 + \lambda)} \quad (24)$$

independent of Γ^+ . The saturated limit is identical to its BCS value except that it includes in addition the renormalization factor $(1 + \lambda)$. It is quite important to note that the existence of this limit has just recently been confirmed experimentally by Taillefer *et al.*³⁰ using optimally doped untwinned YBCO single crystals, a result which is in strong support of a predominantly $d_{x^2-y^2}$ -symmetric order parameter.

Similar manipulations for the conductivity formula (13) give

$$\sigma_1(0,0) = \sigma_{00} = \frac{e^2 N(0)v_F^2}{2} \frac{1}{\pi} \frac{2}{\Delta_0(1 + \lambda)}, \quad (25)$$

which also contains the renormalization factor $(1 + \lambda)$. The Lorenz number $\kappa_{ab,e}/T\sigma_1$ has its free-electron value L_0 in the saturation limit with the above universal value for $\kappa_{ab,e}/T$ and for $\sigma_1(T \rightarrow 0)$. In Fig. 6 (top frame) we show results for the saturated value of L/L_0 at $T=0$ as a function of the strength in the coupling of the electron-boson spectral density $I^2F(\Omega)$, i.e., of T_c/ω_{\log} . In these calculations ω_{\log} was changed by changing the value of ω_{st} in Eq. (8) with I^2 readjusted to keep $T_{c0} = 100$ K. We note from this figure that the Lorenz number in the saturated regime at $T=0$ for resonant scattering depends on the size of T_c/ω_{\log} and recovers its BCS value given by the ratio of Eq. (24) to Eq. (25) only for $T_c/\omega_{\log} \rightarrow 0$. On the other hand, remarkably, the deviations from the ideal value are always very small and can be ignored. Note that the solid squares are calculated from the full formula (9) and (13) with a low-frequency cutoff in $I^2F(\Omega)$ and the open triangles without. At this point it seems to be appropriate to point out that the spectra with the low-frequency cutoff built in do have significantly smaller values for T_c/ω_{\log} . Nevertheless, the corresponding data points have been placed at the T_c/ω_{\log} values of the corresponding spectra without the low-frequency cutoff in an at-

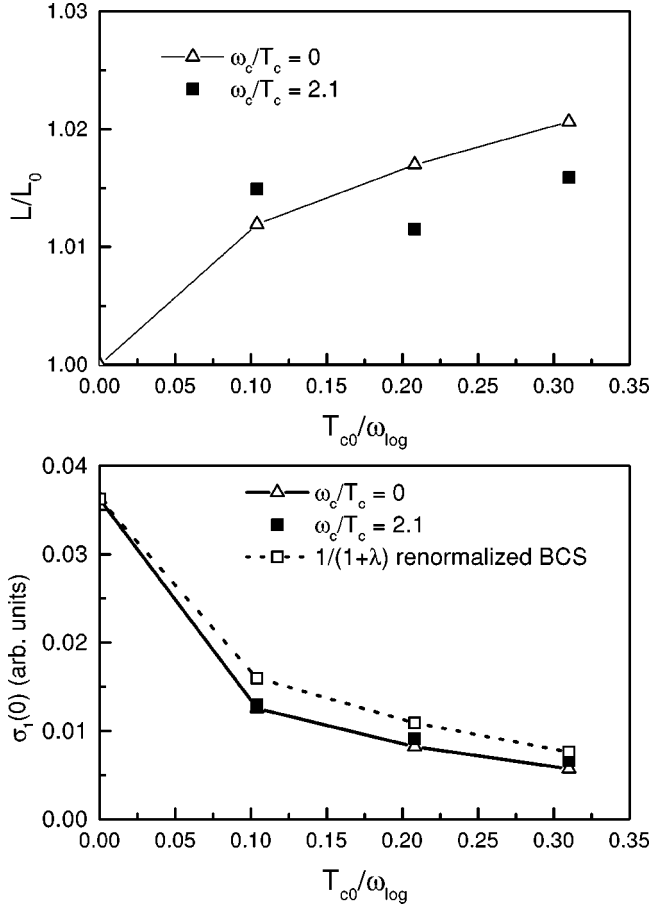


FIG. 6. The coupling dependence of the normalized Lorenz number at $T=4.75$ K (upper frame) and the zero-frequency real part of the optical conductivity (lower frame) as a function of the coupling strength T_{c0}/ω_{log} in the electron-boson spectral density. The open triangles are results without a low-frequency cutoff $\omega_c = 0$ and the solid squares with such a cutoff ($\omega_c = 2.1T_c$). In the lower frame we also compare the results of numerical calculations with the expression $2/\pi\Delta_0(1+\lambda)$ with Δ_0 related to the critical temperature through the BCS relation for d -wave $2\Delta_0/k_B T_c = 4.29$ (open squares). The lines are drawn to guide the eye.

tempt to make the correlation of the data more apparent. In these curves $\Gamma^+/T_{c0} = 0.096$ or $T_c/T_{c0} = 0.95$, with resonant scattering assumed. While the zero-temperature value L/L_0 with resonant scattering is hardly affected by strong coupling effects the bottom frame of Fig. 6 shows that this is not the case when $\sigma_1(0,0)$ and $\kappa_{ab,e}(T)/T$ in the limit $T \rightarrow 0$ are considered separately. Results for $\sigma_1(0,0)$ as a function of T_c/ω_{log} show a large variation, dropping from a value of ~ 0.035 to less than ~ 0.01 as T_c/ω_{log} ranges from 0 (BCS value for $T=0$) to 0.31 (very strong coupling). The solid squares are again the result of full strong-coupling calculations based on the numerical evaluation of Eq. (13) from complete numerical solutions to Eqs. (1) and (2). Γ^+ was adjusted to get $T_c/T_{c0} = 0.95$. Also, a low-frequency cutoff is used in $I^2 F(\Omega)$, while the open triangles involve no cutoff. The results are clearly not dependent significantly on the low-frequency part of the fluctuation spectrum. Finally, we compare with our renormalized BCS result of Eq. (25) which includes the factor $(1+\lambda)$. These are the open squares and we see good agreement with the results of the complete cal-

culations. This demonstrates that for this quantity strong-coupling effects are captured well by the single renormalization $(1+\lambda)$. This of course also holds for the thermal conductivity.

IV. CONCLUSIONS

We have presented calculations of the electronic in-plane thermal conductivity of a $d_{x^2-y^2}$ superconductor which include inelastic scattering at the level of a spectral density that describes the fluctuation spectrum. The choice of spectral density reproduces several of the important properties observed in the cuprates: For example, the quasilinear law for the temperature dependence of the scattering rate in the normal state above T_c , and its size (a few T_c),²⁹ The quasilinear frequency-dependent scattering rate over a very large energy scale extending into the mid-infrared region which is obtained from optical data and its size (of order ν at ν),^{8,29,31,32} The broad nearly constant electronic Raman background³³ of the normal state, as well as other properties. The model can also describe well the measured large peak in the temperature dependence of the microwave conductivity at $T \approx 40$ K in pure samples as well as the effect of Zn and Ni doping in these same quantities.^{8,23} This last phenomenon is associated with a feedback effect of the superconducting phase transition on the fluctuation spectrum which is assumed to become reduced or even possibly fully gapped at low temperatures. This feedback effect is expected in electronic pairing mechanisms. This would be the case for electronic coupling to the spin fluctuations observed at momentum transfer $\mathbf{q} = (\pi, \pi)$. The measured spin susceptibility in optimally doped YBCO does indeed show a gapping in the superconducting state and the emergence of the 41 meV peak.³⁴⁻³⁷

Within the same model and without changing any of the parameters we have calculated, using the appropriate strong-coupling formulas generalized to account for angular dependence of the gap around the Fermi circle in the two-dimensional Brillouin zone and the electronic thermal conductivity, and find good agreement with the in-plane data for YBCO. The observed peak is related to the low-frequency cutoff and corresponds to a radical drop in the inelastic-scattering rate on entering the superconducting state. This is not a novel interpretation but what is different is our method of calculation and our way of including the inelastic scattering. The system is believed to be in the very strong-coupling regime with a strong-coupling parameter $T_c/\omega_{log} = 0.31$. BCS results generalized of course to include the d -wave symmetry of the gap should be quantitative only when $T_c/\omega_{log} \rightarrow 0$. All prior calculations that we are aware of have used a BCS approach and the few that have included the inelastic scattering do so through a temperature-dependent elastic impurity scattering rate with the temperature dependence modeled through consideration of a spin-fluctuation mechanism. We also have a spin-fluctuation mechanism in mind and have used a spectral density with the form expected for the coupling of the quasiparticles to spin fluctuations in a nearly antiferromagnetic Fermi liquid. The precise form of this spectral density could be altered, but at the moment, we do not have a definitive microscopic model of the mechanism involved and cannot make a definitive choice.

Another zero-frequency quantity, very closely related to the thermal conductivity, is the real part of the dc conductivity in the superconducting state and this quantity is closely related to the microwave conductivity. We have studied the effect of elastic impurity scattering in the Born (weak) and the unitary (strong) limit on $\sigma_1(0, T)$ as well as on the thermal conductivity and have compared them in relation to the Lorenz number and the universal saturation of both quantities as $T \rightarrow 0$. The role of strong coupling has been delineated and a simple approximate formula for the saturated value of

the conductivity is given in terms of the boson mass renormalization that enters the theory.

ACKNOWLEDGMENTS

Research was supported in part by the Natural Sciences and Engineering Research Council of Canada (NSERC) and by the Canadian Institute for Advanced Research (CIAR). E.S. acknowledges support by Fonds zur Förderung der wissenschaftlichen Forschung (FWF), Vienna, Austria under Contract No. P11890-NAW.

-
- ¹M. C. Nuss, P. M. Mankiewich, M. L. O'Malley, E. H. Westerwick, and P. B. Littlewood, *Phys. Rev. Lett.* **66**, 3305 (1991).
²D. A. Bonn, P. Dosanjh, R. Liang, and W. N. Hardy, *Phys. Rev. Lett.* **68**, 2390 (1992).
³D. A. Bonn, D. C. Morgan, K. Zhang, R. Liang, D. J. Baar, and W. N. Hardy, *J. Phys. Chem. Solids* **54**, 1297 (1993).
⁴D. A. Bonn, S. Kamal, K. Zhang, R. Liang, D. J. Baar, E. Klein, and W. N. Hardy, *Phys. Rev. B* **50**, 4051 (1994).
⁵D. B. Romero, C. D. Porter, D. B. Tanner, L. Forro, D. Mandrus, L. Mihaly, G. L. Carr, and G. P. Williams, *Phys. Rev. Lett.* **68**, 1590 (1992).
⁶R. C. Yu, M. B. Salamon, J. P. Lu, and W. C. Lee, *Phys. Rev. Lett.* **69**, 1431 (1992).
⁷C. Uher, in *Physical Properties of High T_c Superconductors III*, edited by D. M. Ginsberg (World Scientific, Singapore, 1992).
⁸E. Schachinger, J. P. Carbotte, and F. Marsiglio, *Phys. Rev. B* **56**, 2738 (1997).
⁹V. Ambegaokar and L. Tewordt, *Phys. Rev.* **134**, A805 (1964).
¹⁰V. Ambegaokar and J. Woo, *Phys. Rev.* **139**, A1818 (1965).
¹¹V. Ambegaokar and A. Griffin, *Phys. Rev.* **137**, A1151 (1965).
¹²H. Monien, K. Scharnberg, L. Tewordt, and D. Walker, *Solid State Commun.* **61**, 581 (1987).
¹³P. J. Hirschfeld, P. Wolfe, and D. Einzel, *Phys. Rev. B* **37**, 83 (1988).
¹⁴B. Arfi, H. Bahlouli, and C. J. Pethick, *Phys. Rev. B* **39**, 8959 (1989).
¹⁵M. R. Norman and P. J. Hirschfeld, *Phys. Rev. B* **53**, 5706 (1996).
¹⁶P. J. Hirschfeld and W. O. Putikka, *Phys. Rev. Lett.* **77**, 3909 (1996).
¹⁷J. P. Carbotte, C. Jiang, D. N. Basov, and T. Timusk, *Phys. Rev. B* **51**, 11 798 (1995).
¹⁸J. P. Carbotte and C. Jiang, *Phys. Rev. B* **48**, 4231 (1993).
¹⁹J. P. Carbotte and C. Jiang, *Phys. Rev. B* **49**, 6126 (1994).
²⁰F. Marsiglio, M. Schossmann, and J. P. Carbotte, *Phys. Rev. B* **37**, 4965 (1988).
²¹C. Jiang, E. Schachinger, J. P. Carbotte, D. N. Basov, and T. Timusk, *Phys. Rev. B* **54**, 1264 (1996).
²²J. P. Carbotte, *Rev. Mod. Phys.* **62**, 1027 (1990).
²³E. Schachinger and J. P. Carbotte, *Phys. Rev. B* **57**, 7970 (1998).
²⁴M. Matsukawa, T. Mizukoshi, K. Noto, and Y. Shiohara, *Phys. Rev. B* **53**, R6034 (1996).
²⁵P. A. Lee, *Phys. Rev. Lett.* **71**, 1887 (1993).
²⁶P. J. Hirschfeld, W. O. Putikka, and D. J. Scalapino, *Phys. Rev. Lett.* **71**, 3705 (1993); *Phys. Rev. B* **50**, 10 250 (1994).
²⁷P. J. Hirschfeld and N. Goldenfeld, *Phys. Rev. B* **48**, 4219 (1993).
²⁸M. J. Graf, S. K. Yip, J. A. Sauls, and D. Rainer, *Phys. Rev. B* **53**, 15 147 (1996).
²⁹D. B. Tanner and T. Timusk, in *Physical Properties of High Temperature Superconductors III*, edited by D. M. Ginsberg (World Scientific, Singapore, 1993).
³⁰L. Taillefer, B. Lussier, R. Gagnon, K. Behnia, and H. Aubin, *Phys. Rev. Lett.* **79**, 483 (1997).
³¹A. V. Puchkov, P. Fournier, D. N. Basov, T. Timusk, A. Kapitulnik, and N. N. Kolesnikov, *Phys. Rev. Lett.* **77**, 3212 (1996).
³²A. V. Puchkov, D. N. Basov, and T. Timusk, *J. Phys.: Condens. Matter* **8**, 10 049 (1996).
³³S. L. Cooper, M. V. Klein, B. G. Pazol, J. P. Rice, and D. M. Ginsberg, *Phys. Rev. B* **37**, 5920 (1988).
³⁴J. Rossat-Mignion, L. P. Regnault, P. Burlet, C. Vettier, and J. Y. Henry, *Physica B* **192**, 109 (1993).
³⁵P. Bourges, L. P. Regnault, Y. Sidis, and C. Vettier, *Phys. Rev. B* **53**, 876 (1996).
³⁶H. F. Fong, B. Keimer, P. W. Anderson, D. Reznik, F. Dogan, and I. A. Aksay, *Phys. Rev. Lett.* **75**, 316 (1995).
³⁷P. Bourges, Y. Sidis, L. P. Regnault, B. Hennion, B. Villeneuve, G. Collin, C. Vettier, J. Y. Henry, and J. F. Marucco, *J. Phys. Chem. Solids* **56**, 1937 (1995).